



**HAL**  
open science

# Insight into the true role of hydrogen-carbonate species in CO oxidation over Pd/Al<sub>2</sub>O<sub>3</sub> catalyst using SSITKA-transmission IR technique

Ibrahim Hatoum, Mélissandre Richard, Christophe Dujardin

► **To cite this version:**

Ibrahim Hatoum, Mélissandre Richard, Christophe Dujardin. Insight into the true role of hydrogen-carbonate species in CO oxidation over Pd/Al<sub>2</sub>O<sub>3</sub> catalyst using SSITKA-transmission IR technique. Catalysis Communications, 2023, Catalysis Communications, 179, pp.106684. 10.1016/j.catcom.2023.106684 . hal-04146275

**HAL Id: hal-04146275**

**<https://hal.univ-lille.fr/hal-04146275>**

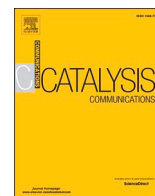
Submitted on 29 Jun 2023

**HAL** is a multi-disciplinary open access archive for the deposit and dissemination of scientific research documents, whether they are published or not. The documents may come from teaching and research institutions in France or abroad, or from public or private research centers.

L'archive ouverte pluridisciplinaire **HAL**, est destinée au dépôt et à la diffusion de documents scientifiques de niveau recherche, publiés ou non, émanant des établissements d'enseignement et de recherche français ou étrangers, des laboratoires publics ou privés.



Distributed under a Creative Commons Attribution - NonCommercial - NoDerivatives 4.0  
International License



# Insight into the true role of hydrogen-carbonate species in CO oxidation over Pd/Al<sub>2</sub>O<sub>3</sub> catalyst using SSITKA-transmission IR technique

Ibrahim Hatoum, Méliandre Richard, Christophe Dujardin \*

Univ. Lille, CNRS, Centrale Lille, Univ. Artois, UMR 8181, UCCS - Unité de Catalyse et Chimie du Solide, 59000 Lille, France

## ARTICLE INFO

**Keywords:**  
CO oxidation  
SSITKA  
*Operando* IR spectroscopy  
Hydrogen-carbonate  
Mechanism  
Palladium

## ABSTRACT

The powerful combination of steady state isotopic transient kinetic analysis (SSITKA) and *operando* infrared spectroscopy (IR) was applied to study the CO oxidation reaction on Pd-supported Al<sub>2</sub>O<sub>3</sub> catalyst at low temperature. The aim was to reveal the true role of hydrogen-carbonate species in the reaction mechanism. The SSITKA-IR experiments, conducted in presence and absence of CO<sub>2</sub> in the gas feed, have confirmed that hydrogen-carbonate species behave as *spectator species* in the reaction. Its formation was due to re-adsorption of the CO<sub>2</sub> product itself on the alumina surface as confirmed by the direct <sup>12</sup>CO<sub>2</sub>/<sup>13</sup>CO<sub>2</sub> exchange observed on the bare support.

## 1. Introduction

Increasing the level of pollution emitted by combustion engine vehicles has been accompanied by a strictness of global regulations to reduce gas emissions. Recently, the European commission has proposed the new Euro-7 standards bringing stricter emission limits for all types of internal combustion engines [1]. Amongst others, carbon monoxide emission standard for gasoline engines has been reduced to half (500 mg per km). In this work, a particular attention was paid to the short trips (5000 mg per trip, <10 km) impacted by cold-start and warm-up driving periods.

In three-way catalytic converters, CO oxidation is mainly catalyzed by supported palladium-based catalytic materials [2–4]. During the last decade, many efforts have been made to acquire a comprehensive knowledge regarding the catalytic chemistry of CO oxidation on Pd [5]. Investigating the nature of active sites and the role of surface adsorbed species formed during the reaction, namely carbonyls, formates, carbonates, and hydrogen-carbonates is critical in order to better understand the mechanism at hand and increase the activity of the catalyst at low temperatures ( $T < 200$  °C). Recently, Murata et al. [6] have demonstrated that linear carbonyls adsorbed on Pd corner sites and Pd (111) facets the latter are highly active sites for CO oxidation at 130 °C. In their infrared spectroscopy investigation, Föttinger et al. [7,8] stated that CO<sub>2</sub> formation can also occur on Pd/alumina via a reaction between CO and hydroxyl groups on the support, whereas CO dissociation does not occur.

The combination of in situ and *operando* analysis techniques are needed to obtain the most accurate information on catalytic mechanisms. Steady State Isotopic Transient Kinetic Analysis (SSITKA) was developed by Happel [9], Bennett [10] and Biloen [11] proposed the combination of the advantages of both steady-state and transient kinetic regimes to better understand reaction mechanistic pathways. Coupled with infrared spectroscopy (IR), SSITKA-IR allows to determine kinetic parameters, as well as the nature of surface-adsorbed active and inactive species during the reaction [12,13]. This technique was applied successfully to confirm the role of hydrogen-carbonates as inactive species formed during CO oxidation reaction on Pt/Al<sub>2</sub>O<sub>3</sub> [14]. The hydrogen-carbonates could then be formed by either spillover of adsorbed CO<sub>2</sub> on the alumina surface or by re-adsorption of gaseous CO<sub>2</sub> at the surface of the alumina support.

In this study, SSITKA-transmission IR experiments were performed to investigate the oxidation of CO on Pd/Al<sub>2</sub>O<sub>3</sub>, trying to elucidate the true involvement of hydrogen-carbonate species in the reaction mechanism at a low temperature.

## 2. Experimental

### 2.1. Catalyst preparation and characterizations

The Pd/Al<sub>2</sub>O<sub>3</sub> catalyst was prepared by the impregnation of  $\gamma$ -Al<sub>2</sub>O<sub>3</sub> support (supplied by the Centre de Recherches de SOLAIZE TOTAL Energies) with Palladium (II) acetylacetonate (Fluka) precursor salt to

\* Corresponding author.

E-mail address: [christophe.dujardin@centralelille.fr](mailto:christophe.dujardin@centralelille.fr) (C. Dujardin).

obtain 1 wt% metal loading. The catalyst was then dried overnight at 85 °C, calcined 4 h under air gas flow at 500 °C, and finally reduced with H<sub>2</sub>(g) at 400 °C/2.5 h. Final Pd loading was determined by ICP-OES 5110 (Agilent Technologies).

Nitrogen physisorption measurements were performed on a Micromeritics TriStar II instrument. The experiments were conducted using 0.2 g of powder sample, previously outgazed at 150 °C under vacuum for 2 h. Brunauer-Emmett-Teller (BET) theory was applied to calculate the specific surface area. Pore size distribution was obtained from the complete isotherms based on the Barret-Joyner-Halenda (BJH) theory.

H<sub>2</sub> chemisorption measurements were carried out at 0 °C in a Micromeritics Autochem II instrument using a pulse technique. Prior to the adsorption, the catalyst (50 mg) was pretreated under 5 vol% H<sub>2</sub>/Ar at 400 °C for 5 h. The temperature of the catalyst sample was then reduced to 0 °C under Ar gas atmosphere in order to perform the chemisorption measurements during which H<sub>2</sub> pulses (5 vol% H<sub>2</sub> in Ar) were injected until saturation. The Pd dispersion was calculated based on the total volume of gas adsorption, assuming a Pd<sub>s</sub>:H ratio of 1.

## 2.2. SSITKA-IR experiments

*Operando* SSITKA-IR measurements were performed using a 7.5 mg square pellet (1.21 cm<sup>2</sup>) of Pd/Al<sub>2</sub>O<sub>3</sub> catalyst. The system is described in the Supporting Information (Fig. S1). Briefly, the pellet was placed in the homemade transmission IR cell (dead volume < 0.5 cm<sup>3</sup>, KBr windows) connected upstream to an automatic pilot system for gas flow and switching valves control.

The catalyst was firstly reduced at 400 °C/5 h under 5% H<sub>2</sub>/He (30 mL min<sup>-1</sup>). Then, the SSITKA-IR study was performed by feeding 12 mL min<sup>-1</sup> of 2000 ppm CO/10% O<sub>2</sub>/He gas mixture to the catalyst. The temperature was increased from 50 °C to 116 °C (1 °C/min). The occurrence of a hysteresis phenomenon is usually reported on noble metals during CO oxidation [15]. Thus, in order to reach steady-state reaction conditions, a 30-min period of isotherm equilibration was first carried out at 116 °C until CO conversion remained stable at 8.5%. The <sup>12</sup>CO reactant was then replaced by 2000 ppm of its labeled counterpart <sup>13</sup>CO at isobaric and isothermal conditions. Three isotopic <sup>12</sup>CO → <sup>13</sup>CO exchange gas switches were repeated to record the concentration evolution of reversibly adsorbed intermediates, and also check reproducibility (a true steady-state was achieved). The complete SSITKA step-gas switching procedure was as follows: 2000 ppm <sup>12</sup>CO/10% O<sub>2</sub>/He → 2000 ppm <sup>13</sup>CO/10% O<sub>2</sub>/5000 ppm Kr/7900 ppm CH<sub>4</sub>/He. Kr and CH<sub>4</sub> were used as inert gas for kinetic analysis (MS) and direct comparison of MS (gas phase) and IR (adsorbed species) signals, respectively. SSITKA-IR analysis was also carried out at the same CO conversion, ca. 8.5%, at 131 °C in the presence of CO<sub>2</sub>. In the latter case, the same experimental procedure was used with the only difference the addition of 2000 ppm of CO<sub>2</sub> in both feed gas streams. Moreover, a CO<sub>2</sub> SSITKA-IR was performed directly on the bare alumina support applying the following step-gas switch: 2000 ppm <sup>12</sup>CO<sub>2</sub>/10% O<sub>2</sub>/He → 2000 ppm <sup>13</sup>CO<sub>2</sub>/10% O<sub>2</sub>/5000 ppm Kr/7900 ppm CH<sub>4</sub>/He at 116 and 131 °C.

Gas phase analysis of the gas composition towards the inlet and from the outlet of IR cell was performed by micro-gas chromatography (µGC Varian 490) and quadrupole mass spectrometry (MS Pfeiffer QMS 200, 70 eV positive electronic impact). The catalytic surface was analyzed by Fourier transformed transmission IR spectroscopy (Thermo Scientific Nicolet 6700) using the rapid-scan mode (1 scan, resolution = 2 cm<sup>-1</sup>) and a N<sub>2</sub>-cooled MCT detector.

The CO conversion ( $\chi_{CO}$ ) was calculated as the percentage ratio between the amount of CO consumed at the considered temperature and the initial CO feed concentration. The surface residence times of surface adsorbed species,  $\tau_{CO}$  (CO-s) and  $\tau_C$  (active carbon-containing intermediates leading to CO<sub>2</sub>) were determined from SSITKA-MS transient response curves by calculating the integral difference between the <sup>13</sup>CO and CH<sub>4</sub> response curves, and that between the <sup>13</sup>CO<sub>2</sub> and <sup>13</sup>CO response

curves, respectively. The concentration of reversibly adsorbed CO ( $N_{CO}$ ), their respective surface coverage ( $\theta_{CO}$ ), and the concentration of C-containing intermediates ( $N_C$ ) were calculated using the following Eqs. (1)–(3) based on material balances [16]:

$$N_{CO}(\mu\text{mol g}_{cat}^{-1}) = \frac{F_T Y_{CO}^f (1 - \chi_{CO})}{W} \tau_{CO} \quad (1)$$

$$N_C(\mu\text{mol g}_{cat}^{-1}) = \frac{F_T Y_{^{13}CO_2}}{W} \tau_C \quad (2)$$

$$\theta_{CO} = N_{CO}/N_{Pd,surf} \quad (3)$$

where  $F_T$  is the total molar flow rate ( $\mu\text{mol s}^{-1}$ ) of the feed gas stream,  $Y_{CO}^f$  is the mole fraction of CO in the feed,  $Y_{^{13}CO_2}$  is the mole fraction of <sup>13</sup>CO<sub>2</sub> at the outlet of the reactor in steady-state,  $W$  is the total mass of the catalyst pellet ( $7.5 \times 10^{-3}$  g), and  $N_{Pd,surf}$  is the molar amount of surface palladium per gram of catalyst ( $\mu\text{mol Pd g}_{cat}^{-1}$ ) calculated from the Pd dispersion and loading values. The steady-state turnover frequency of CO conversion, namely TOF<sub>CO</sub> (s<sup>-1</sup>), was calculated under the <sup>12</sup>CO/O<sub>2</sub>/He feed gas stream before the SSITKA experiment, according to Eq. (4) [17].

$$TOF_{CO} = \frac{r_{CO}}{N_{Pd,surf}} \quad (4)$$

where  $r_{CO}$  is the steady-state rate of CO conversion in  $\mu\text{mol g}^{-1} \text{s}^{-1}$  (the calculation of  $r_{CO}$  is detailed in Supporting Information).

## 3. Results and discussion

### 3.1. Fresh catalyst

The final mass loading of Pd deposited on the alumina support was determined by ICP-OES analysis and was found to be 0.87 wt%. BET analysis showed that the Pd/Al<sub>2</sub>O<sub>3</sub> catalyst developed a high surface area, ca. 235 m<sup>2</sup> g<sup>-1</sup> and a pore volume of 0.79 cm<sup>3</sup> g<sup>-1</sup>, which are comparable to the area and pore volume of the support itself ( $\gamma$ -Al<sub>2</sub>O<sub>3</sub>), i. e. 225 m<sup>2</sup> g<sup>-1</sup> and 0.76 cm<sup>3</sup> g<sup>-1</sup>, respectively. Metal dispersion measured by H<sub>2</sub> chemisorption showed a Pd dispersion value of 71.1% corresponding to a mean Pd particle size of ~1.54 nm (see estimation details in the Supporting Information).

### 3.2. SSITKA-IR for CO oxidation

#### 3.2.1. CO oxidation without CO<sub>2</sub> in the feed gas stream on Pd/Al<sub>2</sub>O<sub>3</sub>

The CO oxidation reaction was first performed without the presence of CO<sub>2</sub> in the feed gas mixture. The transient normalized concentration response curves of CH<sub>4</sub> (tracer gas), <sup>13</sup>CO and <sup>13</sup>CO<sub>2</sub> obtained during the SSITKA switch <sup>12</sup>CO/O<sub>2</sub>/He → <sup>13</sup>CO/O<sub>2</sub>/CH<sub>4</sub>/Kr/He at 116 °C are presented in Fig. 1. The CO conversion here was limited to 8.5% to maintain differential reactor conditions, and the TOF<sub>CO</sub> was estimated to be 0.035 s<sup>-1</sup>. It should be mentioned that the CO conversion is equal to the CO<sub>2</sub> yield, suggesting the absence of coke formation. The results show that the <sup>13</sup>CO transient response curve lags behind that of CH<sub>4</sub> due to the CO converted but also to a detectable concentration of reversibly adsorbed carbonyls (CO-s) formed during the reaction. In the same manner, the transient response curve of <sup>13</sup>CO<sub>2</sub> lags behind that of <sup>13</sup>CO response curve and this is attributed to the slower exchange of <sup>12</sup>C-containing active reaction intermediates formed for their <sup>13</sup>C-labeled counterparts before they lead to the formation of <sup>13</sup>CO<sub>2</sub> (the product of reaction). It is worth to note that both isotopic transient response curves cross each other at the expected normalized value of 0.5, ensuring the right isobaric condition of the exchange (Fig. S2).

According to the SSITKA theory, the areas between the response of CH<sub>4</sub> tracer and <sup>13</sup>CO, and that between the <sup>13</sup>CO and <sup>13</sup>CO<sub>2</sub> correspond to the mean surface residence time  $\tau$  of reversibly adsorbed CO ( $\tau_{CO}$  =

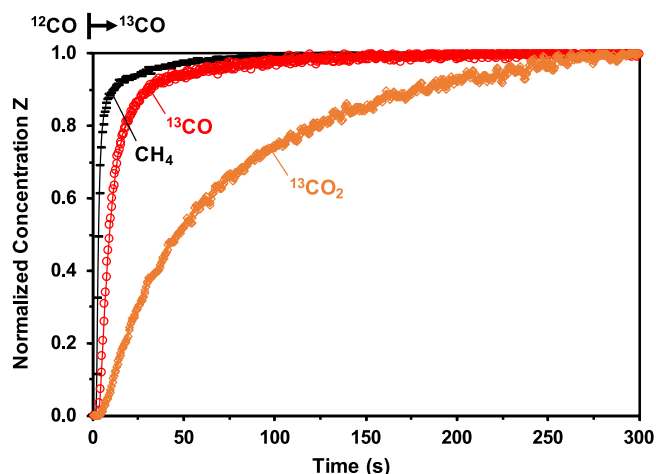


**Fig. 1.** Normalized concentration evolution response curves of  $\text{CH}_4$ ,  $^{13}\text{CO}$  and  $^{13}\text{CO}_2$  during the SSITKA reactant switch:  $^{12}\text{CO}/\text{O}_2/\text{He} \rightarrow ^{13}\text{CO}/\text{O}_2/\text{Kr}/\text{CH}_4/\text{He}$  on  $\text{Pd}/\text{Al}_2\text{O}_3$  at  $116^\circ\text{C}$  ( $\chi_{\text{CO}} = 8.5\%$ ).

8.6 s) and active C-containing intermediates ( $\tau_{\text{C}} = 55.5$  s) leading to  $\text{CO}_2$ , respectively. The surface concentrations and surface coverages of these adsorbed species can be estimated using Eqs. (1)–(3). The estimated values are reported in Table 1. A value for the concentration  $N_{\text{CO}}$  of adsorbed CO-s  $\sim 17.4$   $\mu\text{mol}$  per gram of catalyst was obtained, corresponding to a surface coverage,  $\theta_{\text{CO}}$  (based on Pd) of  $\sim 30\%$ . This value can be compared to the expected CO surface coverage based on a heat of CO adsorption of 29 kcal/mol reported by Szanyi et al. [18]. The theoretical CO surface coverage was estimated to be  $\sim 95\%$  at  $116^\circ\text{C}$  on a bare Pd (100) surface. The lower value of  $\theta_{\text{CO}}$  on Pd found here could be partly explained by the competitive adsorption of oxygen, introduced in large amount, on the Pd surface sites. In addition, the concentration of C-containing intermediates,  $N_{\text{C}}$  was  $\sim 10.4$   $\mu\text{mol}$  per gram of catalyst.

IR transmission spectra were recorded before and after the step-gas switch to determine the chemical nature of adsorbed species during the CO oxidation reaction on  $\text{Pd}/\text{Al}_2\text{O}_3$ . Fig. 2 presents two spectra showing the composition of adsorbed phase on the surface of  $\text{Pd}/\text{Al}_2\text{O}_3$  at  $116^\circ\text{C}$  under the reaction mixtures of  $^{12}\text{CO} + \text{O}_2$  (in black) and  $^{13}\text{CO} + \text{O}_2$  (in red) at the steady state reaction conditions.

In the carbonyl region ( $2200\text{--}1700\text{ cm}^{-1}$ ) shown in Fig. 2a, the IR band observed at  $2088\text{ cm}^{-1}$  (black signal) before the isotopic switch is attributed to linear  $^{12}\text{CO}$  adsorbed on Pd. According to the literature [19,20], linear CO are more likely to be adsorbed on metallic Pd<sup>0</sup> particle corner sites or (111) facets. The larger IR signal observed between 2000 and  $1800\text{ cm}^{-1}$  can be decomposed into several overlapped infrared bands corresponding to bridged and multi-bonded  $^{12}\text{CO}$  adsorbed on palladium [6,21]. After applying the isotopic exchange (Fig. 2a, red curve), a complete red shift of the linear and bridged/multi-bonded CO bands adsorbed on Pd was observed, giving rise to new  $^{13}\text{CO}$  IR bands at 2039 and  $1950\text{--}1750\text{ cm}^{-1}$ , respectively.

The formation of hydrogen-carbonate species on the alumina support is detected in the carbonate region ( $1700\text{--}1200\text{ cm}^{-1}$ ) shown in Fig. 2b. The IR bands at 1657 and  $1439\text{ cm}^{-1}$  seen in the black spectrum, were attributed to the asymmetric and symmetric stretching  $\nu(\text{OCO})$

**Table 1**

Mean residence times,  $\tau$ , concentrations  $N$ , surface coverages,  $\theta$  of adsorbed CO and C-containing intermediates calculated from the SSITKA CO oxidation experiments on  $\text{Pd}/\text{Al}_2\text{O}_3$  with and without the presence of  $\text{CO}_2$  in the feed.

	T ( $^\circ\text{C}$ )	$\tau_{\text{CO}}$ (s)	$N_{\text{CO}}$ ( $\mu\text{mol g}^{-1}$ )	$\theta_{\text{CO}}$ (on Pd)	$\tau_{\text{C}}$ (s)	$N_{\text{C}}$ ( $\mu\text{mol g}^{-1}$ )
Without $\text{CO}_2$	116	8.6	17.4	0.30	55.5	10.4
With $\text{CO}_2$	131	8.2	16.5	0.28	18.6	3.7

vibrations of hydrogen-carbonate species, respectively [7,22,23]. The latter are accompanied by a small band near  $1231\text{ cm}^{-1}$  corresponding to the bending  $\delta(\text{OH})$  vibration. Unfortunately, due to the low extinction coefficient in the stretching OH region, the expected  $\nu(\text{OH})$  band of these species was not clearly observed, as well as the negative OH band due to the consumption of a surface hydroxyl group present on the  $\gamma$ -alumina surface. Upon exchange with  $^{13}\text{CO}$ , the hydrogen-carbonate bands recorded at 1231, 1439 and  $1657\text{ cm}^{-1}$  are in large part red-shifted providing the IR bands centered at 1224, 1400 and  $1613\text{ cm}^{-1}$ , respectively. Another IR band was detected at  $1384\text{ cm}^{-1}$  in both spectra as shown in Fig. 2b, which does not appear to be impacted by the isotopic  $^{12}\text{CO} \rightarrow ^{13}\text{CO}$  exchange, evidencing its spectator nature. In addition, gaseous methane was also detected after the transient exchange with  $^{13}\text{CO}$  (red spectrum) by the appearance of an extremely weak absorbance at  $1305\text{ cm}^{-1}$ .

### 3.2.2. CO oxidation with $\text{CO}_2$ present in the feed gas mixture on $\text{Pd}/\text{Al}_2\text{O}_3$

After adding 2000 ppm of  $^{12}\text{CO}_2$  in both reaction feeds, the SSITKA  $^{12}\text{CO}/\text{O}_2/^{12}\text{CO}_2/\text{He} \rightarrow ^{13}\text{CO}/\text{O}_2/^{12}\text{CO}_2/\text{Kr}/\text{CH}_4/\text{He}$  switch was performed on  $\text{Pd}/\text{Al}_2\text{O}_3$  to investigate again the CO oxidation and the role of co-fed  $\text{CO}_2$ . The normalized transient response curves of  $\text{CH}_4$ ,  $^{13}\text{CO}$  and  $^{13}\text{CO}_2$  following the reactant isotopic switch are plotted as a function of time in Fig. 3. A similar CO conversion as in the previous experiment was maintained ( $\chi_{\text{CO}} = 8.8\%$ ) by increasing the temperature to  $131^\circ\text{C}$ . It is important to note that this increase in temperature will have an impact on the calculated kinetic parameters since the rate constant also increases. This apparent inhibitor effect of  $\text{CO}_2$ , besides the experimental error, is surprising but it might be related to a change in the proportion of carbonyl species at the Pd surface. Such a change could be attributed to hysteresis-like phenomena [15]. Compared to the previous experiment, a similar value of  $\text{TOF}_{\text{CO}}$  was obtained in the presence of  $\text{CO}_2$  in the feed gas stream, ca.  $0.035\text{ s}^{-1}$ .

As a direct effect of adding  $\text{CO}_2$  in the feed gas stream, the area between the two  $^{13}\text{CO}$  and  $^{13}\text{CO}_2$  response curves decreased significantly, corresponding to a mean residence time ( $\tau_{\text{C}}$ ) of 18.6 s (three times lower than the value obtained without  $\text{CO}_2$  co-addition in the reaction feed gas mixture). The concentration of  $^{13}\text{C}$ -containing intermediates ( $N_{\text{C}}$ ) has decreased to the same extent, ca. 3.7  $\mu\text{mol}$  per gram of catalyst. It should be noted that the total number of C-containing intermediates should not change, except for the variation due to the temperature effect, since the pool of C-containing intermediates is simultaneously exchanged under the  $^{12}\text{CO}_2$  co-feeding SSITKA experiment, which is not taken into account in this case. The different kinetic parameters obtained in the presence and absence of  $\text{CO}_2$  are summarized in Table 1.

On the contrary, the presence of  $\text{CO}_2$  did not have a significant impact on the mean surface residence time and the concentration of reversibly adsorbed CO-s. Only a small decrease of  $\tau_{\text{CO}} = 8.2$  s and  $N_{\text{CO}} = 16.5\text{ }\mu\text{mol g}^{-1}$  was observed in the presence of  $\text{CO}_2$  due to the very slight increase in temperature (change in reaction rate constant,  $k$ ) and CO conversion (mainly effect of partial pressure of CO).

The evolution of adsorbed species on the catalytic surface has been followed by transmission IR during the isotopic exchange in order to observe the effect of the presence of  $\text{CO}_2$ . The IR spectra recorded at  $131^\circ\text{C}$  in both  $^{12}\text{CO} + \text{O}_2 + ^{12}\text{CO}_2$  and  $^{13}\text{CO} + \text{O}_2 + ^{12}\text{CO}_2$  steady states are presented in Fig. 4.

Fig. 4a shows the red isotopic shift of the IR bands corresponding to linear, bridged and multi-bonded carbonyls on Pd, ca. from  $2088\text{ cm}^{-1}$  and  $2000\text{--}1800\text{ cm}^{-1}$  to  $2039\text{ cm}^{-1}$  and  $1950\text{--}1750\text{ cm}^{-1}$  range, respectively. In contrast, in the carbonate region, IR bands at 1657, 1439 and  $1231\text{ cm}^{-1}$  (Fig. 4b) previously assigned to hydrogen-carbonates species, were only  $^{12}\text{C} \rightarrow ^{13}\text{C}$  shifted to a very small extent ( $< 1.5\%$ ) in the presence of  $\text{CO}_2$  in the reactant feed gas mixture. Again, no shift was observed for the small IR band appeared at  $1384\text{ cm}^{-1}$ .

### 3.2.3. $\text{CO}_2$ exchange on $\text{Al}_2\text{O}_3$ support

In order to further confirm the formation route of

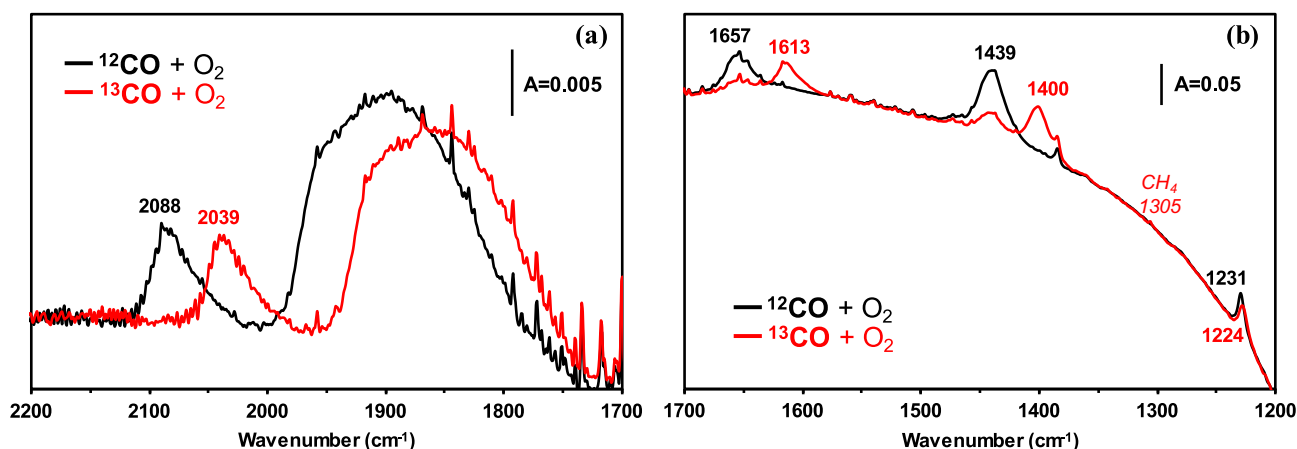


Fig. 2. IR spectra recorded on Pd/Al<sub>2</sub>O<sub>3</sub> during CO oxidation at 116 °C in the presence of <sup>12</sup>CO/O<sub>2</sub>/He (black) and <sup>13</sup>CO/O<sub>2</sub>/Kr/CH<sub>4</sub>/He (red): (a) carbonyl region, and (b) carbonate region.

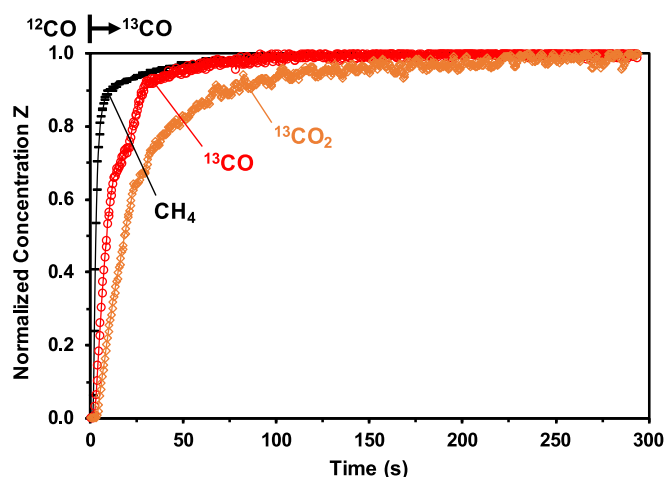


Fig. 3. Normalized concentration evolution response curves of CH<sub>4</sub>, <sup>13</sup>CO and <sup>13</sup>CO<sub>2</sub> obtained following the SSITKA switch in the presence of <sup>12</sup>CO<sub>2</sub>: <sup>12</sup>CO/O<sub>2</sub>/<sup>12</sup>CO<sub>2</sub>/He → <sup>13</sup>CO/O<sub>2</sub>/<sup>12</sup>CO<sub>2</sub>/Kr/CH<sub>4</sub>/He on Pd/Al<sub>2</sub>O<sub>3</sub> at 131 °C ( $\chi_{\text{CO}_2} = 8.8\%$ ).

hydrogen-carbonate species, a <sup>12</sup>CO<sub>2</sub>/<sup>13</sup>CO<sub>2</sub> SSITKA-IR exchange was performed directly on the bare Al<sub>2</sub>O<sub>3</sub> support. The transient normalized concentration response curves of CH<sub>4</sub> and <sup>13</sup>CO<sub>2</sub> obtained on the alumina following the <sup>12</sup>CO<sub>2</sub>/O<sub>2</sub>/He → <sup>13</sup>CO<sub>2</sub>/O<sub>2</sub>/Kr/CH<sub>4</sub>/He switch at 116 and 131 °C are presented in Fig. S3 (Supporting Information). The comparison with previous results of the CO oxidation on Pd/Al<sub>2</sub>O<sub>3</sub> in the presence of CO<sub>2</sub> (Fig. 3) are shown in Fig. 5a. A clear match between both <sup>13</sup>CO<sub>2</sub> profiles (blue and orange curves) was observed, concomitant with the overlapping methane profiles (black and green curves). Similar surface residence times between CH<sub>4</sub> and <sup>13</sup>CO<sub>2</sub> were estimated in both cases, namely:  $\tau_{\text{CO}_2} = 28.8$  s on Al<sub>2</sub>O<sub>3</sub>, and  $\tau_{\text{CO}_2} = 26.7$  s on Pd/Al<sub>2</sub>O<sub>3</sub>.

The evolution of surface adsorbed species has also been followed on bare Al<sub>2</sub>O<sub>3</sub> by transmission IR during the <sup>12</sup>CO<sub>2</sub>/<sup>13</sup>CO<sub>2</sub> isotopic exchange. The IR spectra recorded in the 1700–1200 cm<sup>-1</sup> range in both <sup>12</sup>CO<sub>2</sub>/O<sub>2</sub> and <sup>13</sup>CO<sub>2</sub>/O<sub>2</sub> steady states are presented in Fig. 5b. As previously, <sup>12</sup>C-containing hydrogen-carbonate species formation is detected at 1655, 1442 and 1231 cm<sup>-1</sup> (black spectrum) and which is attributed to the  $\nu(\text{OCO})_{\text{asym}}$ ,  $\nu(\text{OCO})_{\text{sym}}$  and  $\delta(\text{OH})$  vibrations respectively. Hydrogen-carbonates (HCO<sub>3</sub>(ads)) are formed following the Eq. (5), where an OH surface group on the alumina surface interacts with CO<sub>2</sub>.



Upon exchange with <sup>13</sup>CO<sub>2</sub>, the latter bands were red-shifted towards the bands at 1608, 1402 and 1224 cm<sup>-1</sup> (red spectrum),

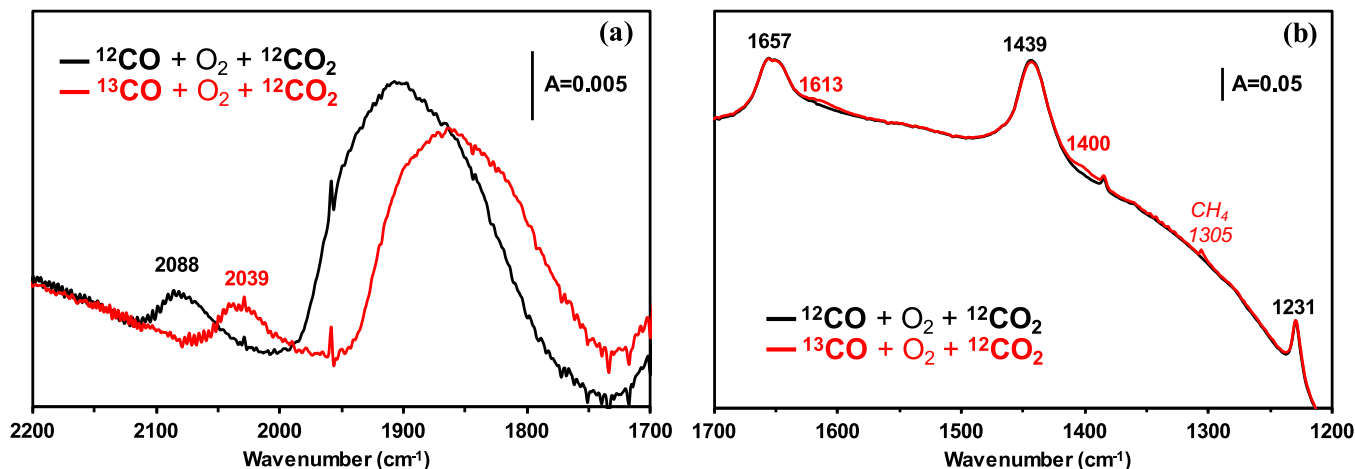


Fig. 4. IR spectra recorded on Pd/Al<sub>2</sub>O<sub>3</sub> during CO oxidation at 131 °C in the presence of <sup>12</sup>CO/O<sub>2</sub>/<sup>12</sup>CO<sub>2</sub>/He (black) and <sup>13</sup>CO/O<sub>2</sub>/<sup>12</sup>CO<sub>2</sub>/Kr/CH<sub>4</sub>/He (red): (a) carbonyl region and (b) carbonate region.

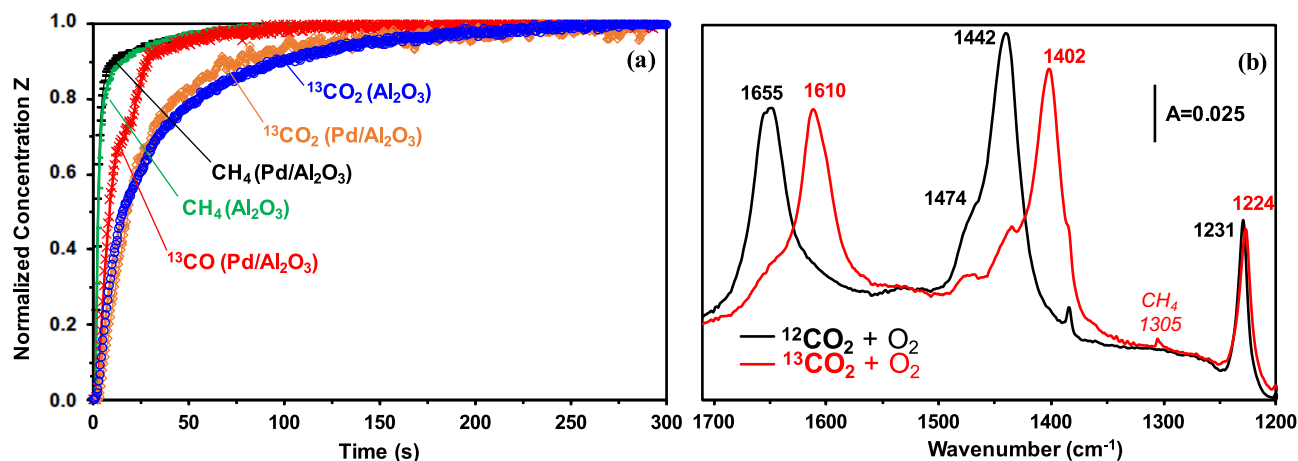


Fig. 5. (a) Comparison of normalized concentration evolution response curves of CH<sub>4</sub> (black), <sup>13</sup>CO (red) and <sup>13</sup>CO<sub>2</sub> (orange) obtained after the <sup>12</sup>CO/O<sub>2</sub>/<sup>12</sup>CO<sub>2</sub>/He → <sup>13</sup>CO/O<sub>2</sub>/<sup>12</sup>CO<sub>2</sub>/Kr/CH<sub>4</sub>/He SSITKA switch on Pd/Al<sub>2</sub>O<sub>3</sub> at 131 °C and of normalized concentration evolution response curves of CH<sub>4</sub> (green) and <sup>13</sup>CO<sub>2</sub> (blue) obtained after the <sup>12</sup>CO<sub>2</sub>/O<sub>2</sub>/He → <sup>13</sup>CO<sub>2</sub>/O<sub>2</sub>/Kr/CH<sub>4</sub>/He SSITKA switch on bare Al<sub>2</sub>O<sub>3</sub> at 131 °C. (b) IR spectra recorded on bare Al<sub>2</sub>O<sub>3</sub> in the carbonate region during <sup>12</sup>CO<sub>2</sub>/<sup>13</sup>CO<sub>2</sub> switch at 131 °C in the presence of <sup>12</sup>CO<sub>2</sub>/O<sub>2</sub>/He (black) and <sup>13</sup>CO<sub>2</sub>/O<sub>2</sub>/Kr/CH<sub>4</sub>/He (red). (For interpretation of the references to colour in this figure legend, the reader is referred to the web version of this article.)

respectively, corresponding to <sup>13</sup>C-containing hydrogen-carbonate species. Difference spectrum was produced and shown in Fig. S3b, which clearly showed the partial disappearance of <sup>12</sup>C-containing hydrogen-carbonate vibrations (negative bands) towards the appearance of their <sup>13</sup>C counterpart. Another IR band appeared at 1474 cm<sup>-1</sup> in both spectra was attributed to unidentate carbonate species. Its intensity decreases after the <sup>13</sup>CO<sub>2</sub> switch but this band doesn't seem to be isotopically shifted towards lower wavenumbers (Fig. S3b, SI). Similar trends were also observed at 116 °C ( $\tau_{\text{CO}_2} = 26.3$  s).

### 3.3. General comments

In this study, the SSITKA technique was successfully coupled to transmission IR spectroscopy in order to elucidate the role of adsorbed species formed on Pd/Al<sub>2</sub>O<sub>3</sub> during the CO oxidation reaction. The measurement of kinetic parameters, such as the mean residence times and concentrations of surface adsorbed species on Pd/Al<sub>2</sub>O<sub>3</sub> have been combined with the determination of their nature. Mainly linear, bridged, and multi-bonded carbonyl-type species were formed during the CO adsorption on metallic Pd<sup>0</sup> at low temperature. The corresponding  $\nu(^{12}\text{C} \equiv \text{O})$  IR bands observed at 2088 cm<sup>-1</sup> and in the 2000–1800 cm<sup>-1</sup> range (Fig. 2a) under <sup>12</sup>CO reactant feed disappeared completely after ~2 min after the isotopic transient switch towards <sup>13</sup>CO, giving rise to the formation of new  $\nu(^{13}\text{C} \equiv \text{O})$  bands at 2039 cm<sup>-1</sup> and 1950–1750 cm<sup>-1</sup>. This trend is consistent with the gas phase evolution of <sup>13</sup>CO observed by mass spectrometry (Fig. S4), where it reached its maximum concentration after 150 s. The fast <sup>12</sup>C → <sup>13</sup>C isotopic exchange of carbonyls observed in SSITKA-IR demonstrates the high exchange of molecularly adsorbed <sup>12</sup>CO-s with gaseous <sup>13</sup>CO and their reactivity towards subsequent reaction intermediates formed in the mechanism of CO oxidation on Pd/Al<sub>2</sub>O<sub>3</sub>.

Initially, the normalized concentrations of <sup>13</sup>CO and <sup>13</sup>CO<sub>2</sub> response curves showed a significant time lag (Fig. 1), indicating that in theory the formation of CO<sub>2</sub> product passes through various active intermediates after CO adsorption on Pd. The *operando* IR results (Fig. 2b) reveal that hydrogen-carbonate species are formed on the alumina surface and follow a <sup>12</sup>C → <sup>13</sup>C isotopic red-shift exchange during the experiment. Other weak absorption bands were also observed by IR on the catalyst surface in the carbonate region but these were clearly identified as *spectator* species in the CO oxidation at low temperatures due to their inability to follow the isotopic exchange. It is worth to note that the <sup>12</sup>C → <sup>13</sup>C exchange of the hydrogen-carbonate species observed

by IR on alumina is very slow compared to surface carbonyl exchange, and even incomplete after 5 min of reaction (Fig. S4–1640 cm<sup>-1</sup> curve). Moreover, this trend is not consistent with the transient response curve recorded for <sup>13</sup>CO<sub>2</sub> product formation by mass spectrometry.

The addition of 2000 ppm of CO<sub>2</sub> in the feed gas stream proved unequivocally against the previous SSITKA-IR conclusion about the active role of hydrogen-carbonate species in CO oxidation reaction on Pd/Al<sub>2</sub>O<sub>3</sub>. Indeed, the presence of CO<sub>2</sub> has led to a drastic reduction (three times) of the amount of <sup>13</sup>C-containing intermediate species ( $N_{\text{C}}$ ) compared to the experiment performed without CO<sub>2</sub> at similar CO conversion. Also, the IR spectra recorded in the presence of CO<sub>2</sub> in the carbonate region (Fig. 4b) show negligible <sup>12</sup>C → <sup>13</sup>C isotopic shift of the IR bands attributed to hydrogen-carbonates. This result confirms clearly in coherence with the kinetic calculation that the hydrogen-carbonate species formed during CO oxidation reaction is only a spectator species, and this *does not* participate in the reaction mechanism of CO<sub>2</sub> formation. This conclusion is also supported by the lag observed in Fig. S4 between the relative rate of exchange of <sup>13</sup>CO<sub>2</sub>-MS signal and the 1640 cm<sup>-1</sup> IR band intensity evolution curve of hydrogen-carbonate species. Therefore, most of the significant time lag firstly observed between <sup>13</sup>CO- and <sup>13</sup>CO<sub>2</sub>-MS signals during the SSITKA experiment without CO<sub>2</sub> in the feed (Fig. 1) could be attributed to the re-adsorption of CO<sub>2</sub>, produced by the CO oxidation, on the surface of the alumina support rather than to the formation of some active intermediate species towards CO<sub>2</sub> formation. The overestimation of SSITKA C-pool due to CO<sub>2</sub> re-adsorption effect was previously reported by Efstathiou [24] in the case of the water-gas shift reaction at high temperature. Similar conclusion was previously obtained for CO oxidation reaction on a Pt-supported alumina catalyst using the same experimental procedure [14]. Linear carbonyls were predominant on the Pt surface in contrast to Pd, where bridged carbonyls were mainly observed. The hydrogen-carbonate species behaved similarly on both Pt/Al<sub>2</sub>O<sub>3</sub> and Pd/Al<sub>2</sub>O<sub>3</sub> catalysts suggesting the re-adsorption of CO<sub>2</sub> on the alumina support rather than a direct spillover from the metal particles. This hypothesis was confirmed in this work by performing <sup>12</sup>CO<sub>2</sub>/<sup>13</sup>CO<sub>2</sub> isotopic exchange experiments on bare alumina (Fig. 5). A direct exchange was observed between <sup>12</sup>C-containing hydrogen-carbonates and their <sup>13</sup>C-labeled counterpart on bare Al<sub>2</sub>O<sub>3</sub> highlighting the lack of metal contribution in this process.

It is also important to note that the value of  $N_{\text{C}}$  did not drop to 0 with the pre-saturation of the surface by CO<sub>2</sub> ( $N_{\text{C}} = 3.7 \mu\text{mol g}^{-1}$ ). This observation means either a partial saturation of alumina with carbonate

species by the use of 2000 ppm of  $^{12}\text{CO}_2$  which would be complemented by the formation and re-adsorption of  $^{13}\text{CO}_2$  during the experiment, or that other C-containing intermediate species could be involved in the CO oxidation mechanism. In the second case,  $N_C$  must then be carefully described as consisting of two pools, namely: (i) spectator hydrogen-carbonates, and (ii) active C-containing intermediate species not of the nature of hydrogen-carbonates.

Carbonyls are likely the main active reaction intermediates (CO-s) identified by IR spectroscopic means. Various types of carbonyls can be identified in this work such as linear or bridged carbonyls. Even if all species follow a similar  $^{12}\text{CO}/^{13}\text{CO}$  isotopic exchange, they are not necessarily involved in the reaction pathway. Indeed, one of them can be a spectator with a fast conversion into the reactive species. This work paves the way for further analysis to discriminate the individual role(s) of each carbonyl species according to their adsorption sites during the CO oxidation reaction, as well as their deactivation process. This will be the aim of further study.

#### 4. Conclusions

A full understanding of CO oxidation mechanism on PGM supported catalysts at low temperature ( $< 200\text{ }^\circ\text{C}$ ) is of great importance in order to improve catalyst efficiency and decrease atmospheric pollution levels. The use of *operando* SSITKA-IR in the current study has provided valuable information into the role of the carbonyl and carbonate species formed at the surface of Pd/Al<sub>2</sub>O<sub>3</sub> catalyst during the CO oxidation reaction. The dynamic exchange between  $^{12}\text{CO} + \text{O}_2$  and  $^{13}\text{CO} + \text{O}_2$  in the presence and absence of CO<sub>2</sub> in the reaction gas mixture revealed a fast isotopic shift of the IR band signals related to various types of carbonyl species adsorbed on metallic Pd, suggesting that at least one of them could be an *active* intermediate in the CO<sub>2</sub> formation. By contrast, hydrogen-carbonate species were finally found to behave like *spectator species* since only negligible isotopic exchange of corresponding IR absorption bands were observed in the presence of CO<sub>2</sub> in the feed gas stream. The lag between the  $^{13}\text{CO}$  and  $^{13}\text{CO}_2$  observed on SSITKA normalized concentration curves (no CO<sub>2</sub> was added in the feed) was then assigned to the re-adsorption of the CO<sub>2</sub> product on the bare alumina support by interaction with a surface hydroxyl group. The direct  $^{12}\text{CO}_2/^{13}\text{CO}_2$  exchange observed on alumina clearly supports this conclusion, indicating the absence of the metal in the formation path of hydrogen-carbonate species.

#### Statements and declarations

The authors have no financial or non-financial interest to disclose. The data generated during the current study are available from the corresponding author on reasonable request.

#### CRediT authorship contribution statement

**Ibrahim Hatoum:** Conceptualization, Data curation, Methodology, Investigation, Writing – original draft. **Mélanie Richard:** Conceptualization, Funding acquisition, Methodology, Investigation, Supervision, Validation, Writing – review & editing. **Christophe Dujardin:** Conceptualization, Funding acquisition, Methodology, Investigation, Supervision, Validation, Writing – review & editing.

#### Declaration of Competing Interest

None.

#### Data availability

Data will be made available on request.

#### Acknowledgements

This work was supported by the Region “Hauts-de-France” (Grant STaRS 2019), Centrale Lille Institut, the Ministère de l'Enseignement Supérieur et de la Recherche (CPER IRENE and CPER ECRIN) and the European Fund for Regional Economic Development.

ICP-OES analyses were performed in the « Spectrométrie par torche à plasma » platform of the Research Federation Michel-Eugène Chevreul hosted by the LASIRE laboratory thanks to Veronique Alaimo. Olivier Gardoll from UCCS laboratory is warmly thanked for H<sub>2</sub> chemisorption experiments.

#### Appendix A. Supplementary data

Supplementary data to this article can be found online at <https://doi.org/10.1016/j.catcom.2023.106684>.

#### References

- [1] Proposal for a regulation of the European Parliament and of the Council on type-approval of motor vehicles and engines and of systems, components and separate technical units intended for such vehicles, with respect to their emissions and battery durability (Euro 7) and repealing Regulations (EC) No 715/2007 and (EC) No 595/2009. <https://eur-lex.europa.eu/legal-content/EN/TXT/?uri=CELEX%3A52022PC0586>, 2022 accessed January 18, 2023.
- [2] A. Satsuma, K. Osaki, M. Yanagihara, J. Ohyama, K. Shimizu, Activity controlling factors for low-temperature oxidation of CO over supported Pd catalysts, *Appl. Catal. B Environ.* 132–133 (2013) 511–518, <https://doi.org/10.1016/j.apcatb.2012.12.025>.
- [3] M. Haneda, M. Todo, Y. Nakamura, M. Hattori, Effect of Pd dispersion on the catalytic activity of Pd/Al<sub>2</sub>O<sub>3</sub> for C<sub>2</sub>H<sub>6</sub> and CO oxidation, *Catal. Today* 281 (2017) 447–453, <https://doi.org/10.1016/j.cattod.2016.05.025>.
- [4] D.Q. Phan, S. Kureti, CO Oxidation on Pd/Al<sub>2</sub>O<sub>3</sub> catalysts under stoichiometric conditions, *Top. Catal.* 60 (2017) 260–265, <https://doi.org/10.1007/s11244-016-0608-9>.
- [5] S.B. Kang, S.J. Han, S.B. Nam, I.-S. Nam, B.K. Cho, C.H. Kim, S.H. Oh, Activity function describing the effect of Pd loading on the catalytic performance of modern commercial TWC, *Chem. Eng. J.* 207–208 (2012) 117–121, <https://doi.org/10.1016/j.cej.2012.06.003>.
- [6] K. Murata, E. Eleeda, J. Ohyama, Y. Yamamoto, S. Arai, A. Satsuma, Identification of active sites in CO oxidation over a Pd/Al<sub>2</sub>O<sub>3</sub> catalyst, *Phys. Chem. Chem. Phys.* 21 (2019) 18128–18137, <https://doi.org/10.1039/C9CP03943K>.
- [7] K. Föttinger, W. Emhofer, D. Lennon, G. Rupprechter, Adsorption and reaction of CO on (Pd–)Al<sub>2</sub>O<sub>3</sub> and (Pd–)ZrO<sub>2</sub>: vibrational spectroscopy of carbonate formation, *Top. Catal.* 60 (2017) 1722–1734, <https://doi.org/10.1007/s11244-017-0852-7>.
- [8] K. Föttinger, R. Schlögl, G. Rupprechter, The mechanism of carbonate formation on Pd–Al<sub>2</sub>O<sub>3</sub> catalysts, *Chem. Commun.* (2008) 320–322, <https://doi.org/10.1039/B713161E>.
- [9] J. Happel, Transient tracing, *Chem. Eng. Sci.* 33 (1978) 1567, [https://doi.org/10.1016/0009-2509\(78\)85214-2](https://doi.org/10.1016/0009-2509(78)85214-2).
- [10] A.T. Bell, L.L. Hegeedus (Eds.), *Catalysis under Transient Conditions*, American Chemical Society, Washington, D. C, 1982, <https://doi.org/10.1021/bk-1982-0178>.
- [11] P. Biloen, Transient kinetic methods, *J. Mol. Catal.* 21 (1983) 17–24, [https://doi.org/10.1016/0304-5102\(93\)80108-7](https://doi.org/10.1016/0304-5102(93)80108-7).
- [12] R. Burch, A.A. Shestov, J.A. Sullivan, A steady-state isotopic transient kinetic analysis of the NO/O<sub>2</sub>/H<sub>2</sub> reaction over Pt/SiO<sub>2</sub> catalysts, *J. Catal.* 188 (1999) 69–82, <https://doi.org/10.1006/jcat.1999.2653>.
- [13] C. Ledesma, J. Yang, D. Chen, A. Holmen, Recent approaches in mechanistic and kinetic studies of catalytic reactions using SSITKA technique, *ACS Catal.* 4 (2014) 4527–4547, <https://doi.org/10.1021/cs501264f>.
- [14] I. Hatoum, N. Bouchoul, M. Richard, C. Dujardin, Revealing origin of hydrogen-carbonate species in CO Oxidation over Pt/Al<sub>2</sub>O<sub>3</sub>: a SSITKA-IR study, *Top. Catal.* (2022), <https://doi.org/10.1007/s11244-022-01722-2>.
- [15] R. Al Soubaihi, K. Saoud, J. Dutta, Critical review of low-temperature CO Oxidation and hysteresis phenomenon on heterogeneous catalysts, *Catalysts*. 8 (2018) 660, <https://doi.org/10.3390/catal8120660>.
- [16] S.L. Shannon, J.G. Goodwin, Characterization of catalytic surfaces by isotopic-transient kinetics during steady-state reaction, *Chem. Rev.* 95 (1995) 677–695, <https://doi.org/10.1021/cr00035a011>.
- [17] J.J. Spivey, G.W. Roberts, J.G.G. Jr, S. Kim, W.D. Rhodes, Turnover frequencies in metal catalysis: Meanings, functionalities and relationships, *Catalysis* (2004) 320–348, <https://doi.org/10.1039/9781847553294-00320>.
- [18] J. Szanyi, D.W. Goodman, C.O. Oxidation, on Palladium., 1. A combined kinetic-infrared reflection absorption spectroscopic study of Pd(100), *J. Phys. Chem.* 98 (1994) 2972–2977, <https://doi.org/10.1021/j100062a038>.
- [19] J. Szanyi, J.H. Kwak, Dissecting the steps of CO<sub>2</sub> reduction: 1. The interaction of CO and CO<sub>2</sub> with  $\gamma$ -Al<sub>2</sub>O<sub>3</sub>: an in situ FTIR study, *Phys. Chem. Chem. Phys.* 16 (2014) 15117–15125, <https://doi.org/10.1039/C4CP00616J>.

- [20] J. Xu, L. Ouyang, W. Mao, X.-J. Yang, X.-C. Xu, J.-J. Su, T.-Z. Zhuang, H. Li, Y.-F. Han, Operando and kinetic study of low-temperature, lean-burn methane combustion over a Pd/ $\gamma$ -Al<sub>2</sub>O<sub>3</sub> catalyst, *ACS Catal.* 2 (2012) 261–269, <https://doi.org/10.1021/cs200694k>.
- [21] S.D. Ebbesen, B.L. Mojet, L. Lefferts, The influence of water and pH on adsorption and oxidation of CO on Pd/Al<sub>2</sub>O<sub>3</sub>—an investigation by attenuated total reflection infrared spectroscopy, *Phys. Chem. Chem. Phys.* 11 (2009) 641–649, <https://doi.org/10.1039/B814605E>.
- [22] S. Ojala, N. Bion, S. Rijo Gomes, R.L. Keiski, D. Duprez, Isotopic oxygen exchange over Pd/Al<sub>2</sub>O<sub>3</sub> catalyst: study on C<sup>18</sup>O<sub>2</sub> and <sup>18</sup>O<sub>2</sub> exchange, *ChemCatChem.* 2 (2010) 527–533, <https://doi.org/10.1002/cctc.201000033>.
- [23] G. Busca, E. Finocchio, V.S. Escribano, Infrared studies of CO oxidation by oxygen and by water over Pt/Al<sub>2</sub>O<sub>3</sub> and Pd/Al<sub>2</sub>O<sub>3</sub> catalysts, *Appl. Catal. B Environ.* 113–114 (2012) 172–179, <https://doi.org/10.1016/j.apcatb.2011.11.035>.
- [24] A.M. Efstathiou, Elucidation of mechanistic and kinetic aspects of water-gas shift reaction on supported Pt and Au catalysts via transient isotopic techniques, *Catalysis* 28 (2016) 175–236, <https://doi.org/10.1039/9781782626855-00175>.